

Figure 12 (a,b) Simulated and experimental S_{11} plot of the single-feed cavity containing perspex block with feed location WG4, according to Fig. 8

Presented results completely confirm applicability of TLM method for an analysis of resonant mode distribution inside the real microwave applicator, taking into account the influence of the feed position and the load presence on the resonant frequencies.

REFERENCES

1. T.G. Mihran, Microwave oven mode tuning by slab dielectric loads, *IEEE Trans Microwave Theor Tech* 26 (1987), 381–387.
2. K.S. Kunz and R.J. Luebbers, *The finite difference time domain for electromagnetics*, CRC Press, Boca Raton, FL, 1993.
3. C. Christopoulos, *The transmission-line modelling method*, IEE/OUP Press, 1995.
4. F. Liu, I. Turner, and M.E. Bialkowski, A finite-difference time-domain simulation of power density distribution in a dielectric loaded microwave cavity, *J Microwave Power Electromagn Energy* 29 (1994), 138–148.
5. D.H. Choi and W.J.R. Hoefer, The finite-difference-time-domain method and its application to eigenvalue problems, *IEEE Trans Microwave Theor Tech* 34 (1986), 1464–1470.
6. R.A. Desai, et al, Computer modelling of microwave cooking using the transmission-line model, *IEE Proceedings A* 139 (1992), 30–37.
7. D.C. Dibben and A.C. Metaxas, Finite element time domain analysis

of multimode applicators using edge elements, *J Microwave Power Electromagn Energy* 29 (1994), 242–251.

8. A. Baysar, J.L. Kuester, and S. El-Ghazaly, Theoretical and experimental investigations of resonance frequencies in a microwave heated fluidized bed reactor, *IEEE MTT-S Digest* 3 (1992), 1573–1576.
9. S. Ivkovic, B. Milovanovic, A. Marincic, and N. Doncov, Theoretical and experimental investigations of resonance frequencies in loaded cylindrical microwave cavity, In: *Proceedings of the Third IEEE TELSIS'97 Conference*, Nis, Yugoslavia, 1997, pp. 306–309.
10. B. Milovanovic, N. Doncov, and A. Atanaskovic, Tunnel type microwave applicator analysis using the TLM method, In: *Proceedings of the Fourth International Workshop on Computational Electromagnetics in the Time Domain: TLM/FDTD and Related Techniques*, CEM-TD 2001, Nottingham, UK, 2001, pp. 77–84.
11. B. Milovanovic and N. Doncov, TLM modelling of the circular cylindrical cavity loaded by lossy dielectric sample of various geometric shapes, *J Microwave Power Electromagn Energy* 37 (2002), 237–247.
12. V. Trenkic, A.J. Wlodarczyk, and R. Scaramuzza, Modelling of coupling between transient electromagnetic field and complex wire structures, *Int J Numer Model Electron Network Dev Field* 12 (1999), 257–273.
13. B. Milovanović, A. Marinić, N. Dončov, V. Marković, J. Joković, and A. Atanasković, Analysis of real feed probe influence to the resonant frequencies and field distribution in the cylindrical metallic cavity using 3D TLM method, *Proceedings of Sixth TELSIS Conference*, Nis, Serbia and Montenegro, 2003, pp. 223–228.
14. J. Joković, B. Milovanović, and N. Dončov, TLM analysis of cylindrical metallic cavity excited with a real feed probe, *Int J RF Microwave Comput Aided Eng*, 16 (2006), 346–354.
15. V. Trenkic, The development and characterization of advanced nodes for TLM method, Ph.D. Thesis, University of Nottingham, 1995.
16. A. Ruddle, D. Ward, R. Scaramuzza, and V. Trenkic, Development of thin wire models in TLM, *IEEE International Symposium on Electromagnetic Compatibility*, August 24–28, Denver, CO, 1998, pp. 196–201.
17. T.V.C.T. Chan and H. C. Reader, *Understanding microwave heating cavities*, Artech House, Boston, London, 2000.

© 2006 Wiley Periodicals, Inc.

FIBRE BRAGG GRATING INTERROGATION BASED ON HIGH-BIREFRINGENCE FIBRE LOOP MIRROR FOR STRAIN-TEMPERATURE DISCRIMINATION

O. Frazão,¹ L. M. Marques,² and J. M. Baptista²

¹ INESC Porto
Unidade de Optoelectrónica e Sistemas Electrónicos
Rua do Campo Alegre 687
4169–007 Porto, Portugal
² Universidade da Madeira
Departamento de Matemática e Engenharias
Universitário da Penteada
9000–390 Funchal, Portugal

Received 3 April 2006

ABSTRACT: In this work, we present a fiber Bragg grating interrogation based on high-birefringence fiber loop mirror for strain-temperature discrimination. Due to spectral response of the optical filters it is possible to determine the variation of the wavelength and the optical power of the Bragg grating sensor when subject to strain or temperature. Maximum errors of $\pm 0.4^\circ\text{C}$ and $\pm 12\ \mu\epsilon$ are reported over 80°C and $2000\ \mu\epsilon$ measurement ranges. © 2006 Wiley Periodicals, Inc. *Microwave Opt Technol Lett* 48: 2326–2328, 2006; Published online in Wiley InterScience (www.interscience.wiley.com). DOI 10.1002/mop.21894

1. INTRODUCTION

Fiber Bragg gratings (FBG) were studied and applied in the last years as a sensing element or as an optical filter for optical communications. One of the most explored areas is the monitoring of physical parameters, namely strain and temperature for different engineering applications. Nevertheless, one of the restraints is its cross-sensitivity between both parameters. In order to solve this problem, several configurations of sensing heads were developed [1]. Usually, these sensing heads use two Bragg grating structures written on different optical fibers [2, 3].

The possibility of using a single Bragg grating structure is under intense investigation and one of the alternative solutions is the writing of the Bragg grating in a high birefringence fiber. This approach shows two signatures, from which it is possible to use for simultaneous measurement of strain and temperature [4].

Another solution is to make use of interrogation techniques that allow extracting information beyond the wavelength signature. An interesting analysis is the variation of optical power with the physical parameter. However, to vary the optical power, it is necessary to place an optical filter with a linear decay before or after the sensor reading.

On the other hand the optical fiber-loop mirror [5] has been deeply studied and used in several applications, namely in optical communications like a terahertz optical asymmetric demultiplexer [6] or a nonlinear optical loop mirror [7]. In the optical sensor, it has been used as a Sagnac interferometer for temperature measurement [8] and as an interrogation device for FBG sensors [9].

This work demonstrates experimentally an interrogation technique for Bragg grating sensors using a high-birefringence fiber-loop mirror for strain and temperature discrimination. When the sensing head was subject to an external physical parameter, the Bragg wavelength changed and the optical intensity of the FBG varied due to the spectral response of the filter. With only these two parameters, we are able to measure strain and temperature simultaneously using a single Bragg grating structure.

2. EXPERIMENTAL SETUP

Figure 1 presents the experimental setup which consists in a broadband source, a high-birefringence (HiBi) fiber-loop mirror, an optical circulator (OC) and a FBG sensor. The Bragg grating is centered for a wavelength of ≈ 1545 nm and has 99% reflectivity. It was written using the following standard optical fiber: SMF28, simple germanosilicate core (diameter $8.2 \mu\text{m}$), 3 mol% GeO_2 ,

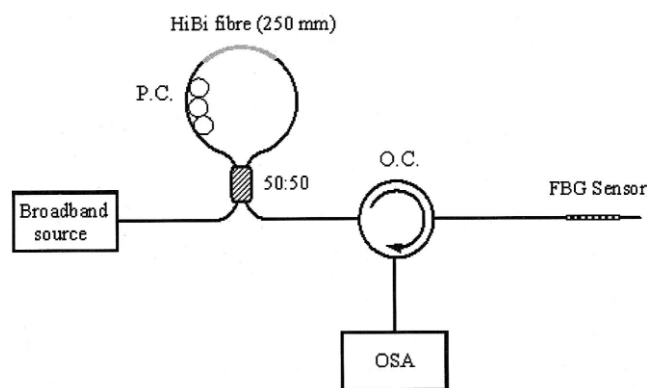


Figure 1 Experimental setup

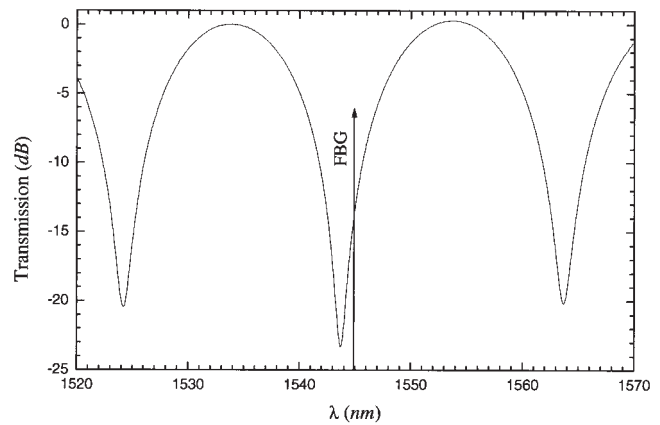


Figure 2 Band pass filter spectral behavior. The filter is formed by a fibre loop mirror with a section of 250 mm HiBi fibre

cold hydrogenated at 100 atm. The FBG sensor was fabricated using a 10 mm length diffractive phase mask ($\Lambda = 1067$ nm) illuminated with a KrF laser operating at 248 nm.

The OC allows the analysis of the light reflected from the FBG. An optical spectrum analyzer (OSA) with a resolution of 0.1 nm was used. The optical source is an erbium-doped broadband source and has the purpose of characterizing the sensing head and it presents a spectral bandwidth of 100 nm and an average wavelength of 1550 nm.

A 3-dB optical coupler with low insertion loss, a fiber-loop with a 250 mm HiBi fiber section and an optical polarization controller (PC) forms the optical fiber-loop mirror. This HiBi fiber (3M FS-PM-7621) is described as a 1550 nm polarization maintaining single mode optical fiber (internal elliptical cladding) with a beat length at 633 nm of 1.6 mm and an attenuation of 1.0 dB/km. The fiber-loop mirror is located between the broadband source and the OC, however, it can be positioned between the OC and the OSA.

3. EXPERIMENTAL RESULTS

The HiBi fiber-loop mirror acts like a band pass filter for the input signal. The difference between the optical path, introduced by the HiBi fiber section, for the two counter propagating waves as they transverse the loop results in constructive and destructive interference which can be seen in the filter response (see Fig. 2). Therefore, the loop filter characteristic is similar to an unbalanced Mach-Zehnder. This filter response was optimized for a spectral width of ≈ 19 nm. The length used for the HiBi fiber was approximately 250 mm according to $\Delta\lambda = \lambda^2/\beta L$ [1] where $\Delta\lambda$ is the filter spectral width, λ is the average wavelength, β is the birefringence, and L is the length of the HiBi optical fiber. The wavelength of the FBG sensor is located in the linear region of the optical filter spectrum, where the slope is approximately $54 \mu\text{W}/\text{nm}$.

The sensing head was attached to a translation stage (TS) with a resolution of $1 \mu\text{m}$ and placed over a thermoelectric cooler device (TEC), which permits the temperature of the sensing head to be set with an error smaller than 0.1°C .

Figures 3 and 4 show the evolution of the wavelength shift ($\Delta\lambda$) and optical power change (ΔP) of the FBG when the sensing head is subject to temperature and strain variation, respectively. The peak wavelength changes accordingly with what is usual for a single FBG. On the other hand, the optical power varies with the slope of the fiber-loop mirror spectral response.

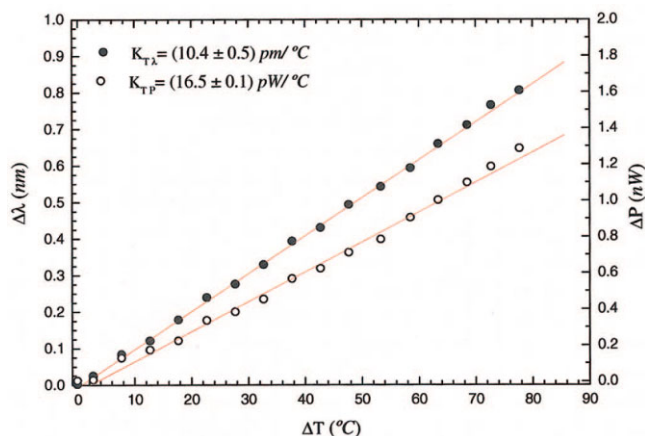


Figure 3 Temperature response of the sensing head [Color figure can be viewed in the online issue, which is available at www.interscience.wiley.com]

These results permit to write a well-conditioned system of two equations for ΔT and $\Delta \varepsilon$ given in a matrix form as:

$$\begin{bmatrix} \Delta T \\ \Delta \varepsilon \end{bmatrix} = \frac{1}{D} \begin{bmatrix} K_{\varepsilon P} & -K_{\varepsilon \lambda} \\ -K_{TP} & K_{T\lambda} \end{bmatrix} \begin{bmatrix} \Delta \lambda \\ \Delta P \end{bmatrix}, \quad (1)$$

where the determinant is $D = K_{TP}K_{\varepsilon \lambda} - K_{\varepsilon P}K_{T\lambda}$. The thermal sensitivity (K_{TP} , $K_{T\lambda}$) and strain sensitivity ($K_{\varepsilon P}$, $K_{\varepsilon \lambda}$) are the sensor head sensitivity coefficients. The matrix coefficients are obtained from the experimental slopes shown in Figures 3 and 4, resulting in

$$\begin{bmatrix} \Delta T \\ \Delta \varepsilon \end{bmatrix} = \frac{1}{6.37} \begin{bmatrix} 2.03 & -0.89 \\ -16.54 & 10.39 \end{bmatrix} \begin{bmatrix} \Delta \lambda \\ \Delta P \end{bmatrix}, \quad (2)$$

with $\Delta \lambda$ in nm, ΔP in nW, ΔT in °C and $\Delta \varepsilon$ in $\mu\varepsilon$ (microstrain). The system performance was evaluated when the sensing head was simultaneously subjected to temperature and strain changes over ranges of 80 °C and 2000 $\mu\varepsilon$, respectively. The maximum error was found to be $\pm 0.4^\circ\text{C}$ and $\pm 12 \mu\varepsilon$, correspondingly.

4. CONCLUSIONS

A sensing head based on Bragg grating technology for simultaneous measurement of strain and temperature was described. It is

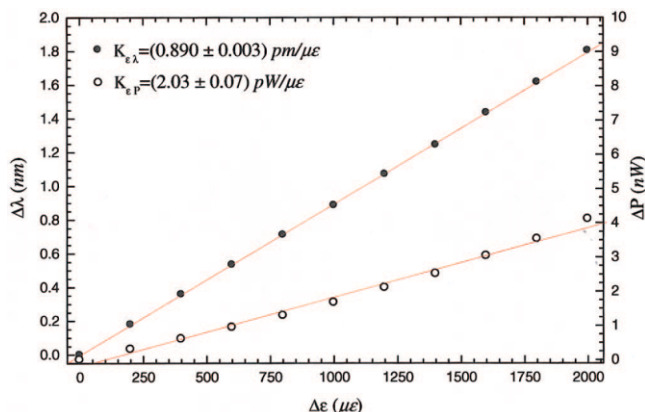


Figure 4 Strain response of the sensing head [Color figure can be viewed in the online issue, which is available at www.interscience.wiley.com]

based on the combination of a single Bragg grating written in standard optical fiber and interrogated through a HiBi fiber-loop mirror. Particular features of this configuration were analyzed and the maximum errors for temperature and strain measurements were found to be $\pm 0.4^\circ\text{C}$ and $\pm 12 \mu\varepsilon$, respectively.

Finally, an advantage of this configuration which uses a HiBi fiber-loop mirror is to interrogate an array FBG with capability to discriminate simultaneously the strain and the temperature.

REFERENCES

- O. Frazão, L.A. Ferreira, F.M. Araujo, and J.L. Santos, Applications of fiber optic grating technology to multi-parameter measurement. *Fiber Integrated Optic* 24 (2005), 227–244.
- S.W. James, M.L. Dockney, and F.P. Tatam, Simultaneous independent temperature and strain measurement using in-fibre Bragg grating sensors, *Electron Lett* 32 (1996), 1133, 1134.
- P.M. Cavaleiro, F.M. Araújo, L.A. Ferreira, J.L. Santos, and F. Farahi, Simultaneous measurement of strain and temperature using Bragg gratings written in germanosilicate and boron-Codoped germanosilicate fibers, *IEEE Photon Tech Lett* 11 (1999), 1635–1637.
- E. Udd, D. Nelson, C. Lawrence, J.R. Spingarn, and B. Ferguson, Three axis strain and temperature sensor, In: *Proceedings of the 11th international conference on optical fiber sensors*, Japan, May 1996, pp. 244–247.
- D.B. Mortimore, Fiber Loop Reflectors, *J Lightwave Tech* 6 (1988), 1217–1224.
- J.P. Sokoloff, P.R. Prucnal, I. Glesk, and M. Kane, A terahertz optical asymmetric demux (TOAD), *IEEE Photon Tech Lett* 5 (1993), 787–790.
- N.J. Doran and D. Wood, Nonlinear-optical loop mirror, *Opt Lett* 13 (1988), 56–58.
- A.N. Starodumov, L.A. Zenteno, D. Monzon, and E. De La Rosa, Fiber Sagnac interferometer temperature sensor, *Appl Phys Lett* 70 (1997), 19–21.
- S. Chung, J. Kim, B.-A. Yu, B. Lee, A fiber bragg grating sensor demodulation technique using a polarization maintaining fiber loop mirror, *IEEE Photon Lett* 13 (2001), 1343–1346.

© 2006 Wiley Periodicals, Inc.

A COMPACT MICROSTRIP BANDPASS FILTER USING FOLDED PARALLEL-COUPLED-LINES

Jian-Zhong Gu^{1,2} and Xiao-Wei Sun¹

¹ Shanghai Institute of Microsystem and Information Technology of Chinese Academy of Sciences
Shanghai 200050, China

² Graduate School of Chinese Academy of Sciences
Beijing 100039, China

Received 12 April 2006

ABSTRACT: A bandpass filter using spiral parallel-coupled-lines is presented for size reduction. Based on the conventional parallel-coupled-line structures, different folded number and coupling structures are proposed for comparison. The band-pass filter with three cells in series is constructed operating from 1.8 GHz to 2.5 GHz. The upper stop-band suppression at 200 MHz offset is more than 30 dB. The band-pass filter size is 70% smaller. © 2006 Wiley Periodicals, Inc. *Microwave Opt Technol Lett* 48: 2328–2330, 2006; Published online in Wiley InterScience (www.interscience.wiley.com). DOI 10.1002/mop.21949

Key words: bandpass filter; parallel-coupled-lines; miniaturization

1. INTRODUCTION

The microstrip parallel-coupled-line filter [1] has been widely used in microwave and wireless systems. This topology of filter is